CO_2-catalyzed efficient dehydrogenation of amines with detailed mechanistic and kinetic studies

Article

CO2-Catalyzed Efficient Dehydrogenation of Amines with Detailed Mechanistic and Kinetic Studies

Daniel Riemer, Waldemar Schilling, Anne Goetz, Yu Zhang, Sascha Gehrke, Igor Tkach, Oldamur Hollóczki, and Shoubhik Das

ACS Catal., **Just Accepted Manuscript** • DOI: 10.1021/acscatal.8b03059 • Publication Date (Web): 29 Oct 2018

CO_2-Catalyzed Efficient Dehydrogenation of Amines with Detailed Mechanistic and Kinetic Studies

Daniel Riemer[a], Waldemar Schilling[a], Anne Goetz[a], Yu Zhang[a], Sascha Gehrke[b], Igor Tkach[c], Oldamur Hollóczki[b], Shoubhik Das[a]*

[a]Institut für Organische und Biomolekulare Chemie, Georg-August-Universität Göttingen, Tammannstraße 2, 37077 Göttingen, Germany.

[b]Mulliken Center for Theoretical Chemistry, Institut für Physikalische und Theoretische Chemie, Universität Bonn, Beringstraße 4+6, 53115 Bonn, Germany.

[c]Research Group EPR Spectroscopy, Max Planck Institute for Biophysical Chemistry, Am Faßberg 11, 37077 Göttingen, Germany.

ABSTRACT: CO_2-Catalyzed dehydrogenation of amines has been achieved under photocatalytic conditions. With this concept, various amines have been selectively dehydrogenated to the corresponding imines in the presence of different functional groups such as nitrile, nitro, ester, halogen, ether, thioether, carbonyl or carboxylic acid moieties. At the end, the CO_2-catalyzed synthesis of pharmaceutical drugs has been achieved. The radical anion from CO_2 has been detected by EPR spectroscopy using DMPO and the mechanism of this reaction is proposed on the basis of DFT calculations and experimental evidences.

KEYWORDS: amines • imines • CO_2 • dehydrogenation • photocatalysts • metal-free

INTRODUCTION

CO_2 is an easily available and sustainable carbon resource that is nontoxic, nonflammable and renewable.[1] However, its high thermodynamic stability and kinetic inertness apply strict conditions for further applications. So far, CO_2 has been thermally, electrochemically and photochemically reduced to formic acid, formaldehyde, methane, CO etc.[2] Reactive substrates such as epoxides, alcohols, amines, alkynes, alkenes and others formed new C-O, C-N, and C-C bonds utilizing CO_2 as a C1 source.[1,3] Strong efforts are also paid to synthesize carboxylic acids and their derivatives *via* C-H bond functionalizations or C-X bond transformations.[4] Parallel to these, utilizing CO_2 as a catalyst or as a mediator for chemical transformations is flourishing rapidly as toxic chemicals can be replaced in this way. Using this concept catalytic rearrangement of propargyl alcohols into *α,β*-unsaturated ketones, C–H bond arylation reactions, allylation *via* cross-coupling reactions, asymmetric allylation reactions of ketones, oxidative dehydrogenation of alkanes and alkyl aromatics, etc. have been achieved.[5]

Inspired by these, we have also discovered the CO_2-catalyzed oxidation of benzylic and allylic alcohols which replaced toxic promoters known for alcohol oxidation by CO_2.[6] To extend this concept, we became keen on finding suitable catalysts for the dehydrogenation of amines. In general, imines are highly important functional groups and have shown wide applications in organic syntheses, pharmaceutical chemistry, agrochemistry and many more.[7] Moreover, imines can also be used as intermediates for further syntheses of natural products and others. However, our efforts for CO_2-catalyzed dehydrogenation of amines to imines did not work in the same way of alcohol oxidation. High temperature or higher base loadings and screening of different bases did not improve the formation of imine. We rationalized that under operationally simple photocatalytic conditions, CO_2 can be transformed into radical species (namely, carbon dioxide radical anion or hydroxycarbonyl radical species) and that should enhance this reaction.[8] In this regard, it should be noted that the generation of these radical species from CO_2 requires special equipment or strict reaction conditions.[9] However, small organic molecule such as pyridine trapped these radicals under mild electrochemical and photochemical conditions and finally were applied these into hydrocarbon-based fuel synthesis.[8] Inspired by this, we became interested to use small organic molecules (pyridine, 1,8-diazabicyclo[5.4.0]undec-7-ene, 1,5-diazabicyclo[4.3.0] non-5-ene etc.) as trapping agents under photocatalytic conditions.[10]

Our main interest was to find a metal-free photocatalyst as they have shown prior activity in CO_2-based transformations towards hydrocarbon fuels and indeed these catalysts are non-toxic, cheaper in price and commercially available.[11] Additionally, metal-free catalysts are more interesting for the pharmaceutical industries due to the easier purifications and to avoid toxic residues in the final product. Traditional methods for the dehydrogenation of amines to imines usually rely on (over-) stoichiometric amount of oxidants such as DDQ, sulfur or peroxides, high temperature, expensive noble or rare earth metals and exhibit poor functional group tolerances.[12] Catalytic methods are also known however requires expensive transition metals such as supported Au catalysts or homogeneous Pd-, Rh-, Ru- or Co-based catalysts, and (over)stoichiometric amount of additives.[7g,13] Considering all

thsese facts and to develop our own interest to promote CO_2-catalyzed reactions, herein we describe metal-free CO_2-catalyzed dehydrogenation of amines to imines.[14]

RESULTS AND DISCUSSION

At the outset of our investigations, different metal-free photocatalysts were applied to optimize the reaction conditions with 1,8-diazabicyclo[5.4.0]undec-7-ene (DBU) as trapping agent and dimethyl sulfoxide (DMSO) as solvent for the transformation of benzyl aniline to benzylidene aniline (**Table S1**). The reaction took place under CO_2 balloon and at room temperature under 12 W LED blue visible-light irradiation. Four different photocatalysts such as fluorescein, rose bengal, 9,10-dicyanoanthracene and eosin Y were investigated for this reaction and among them, eosin Y exhibited 45% yield of the benzylidene aniline. Further screening of different trapping agents resulted in 70% yield of the desired product in the presence of 1,5-diazabicyclo [4.3.0]non-5-ene (DBN). Increasing the DBN amount from 1.0 to 1.2 equivalents (eq.) finally raised the yield to 86% within 24 h. Expediently, this dehydrogenation reaction was also possible in the presence of catalytic amount of CO_2 (20 mol%) with slightly lower yield compared to the optimized reaction conditions.

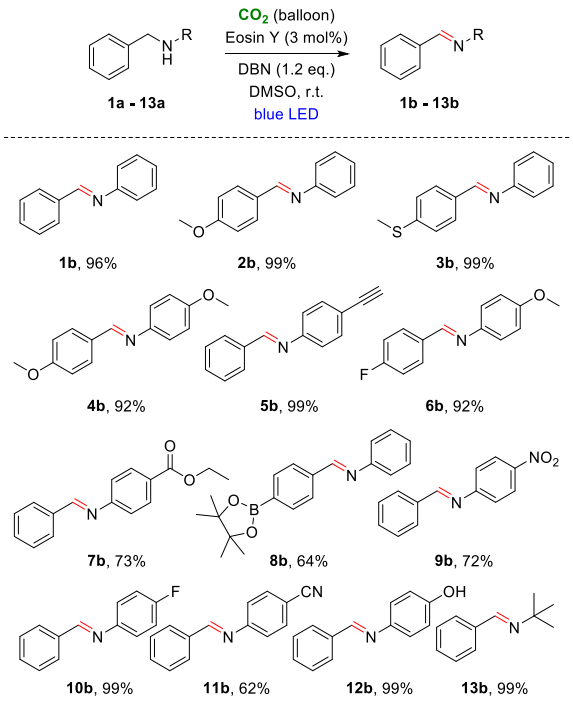

Reaction conditions: Substrate (0.134 mmol), eosin Y (3 mol%), DBN (1.2 eq.), DMSO (2.5 mL), CO_2 (balloon), 12 W blue LED, r.t., 48 h. All are isolated yields.

Scheme 1. Substrates scope for the CO_2-catalyzed dehydrogenation of acyclic amines

With these optimized reaction conditions in hand, we investigated a plethora of acyclic amines to dehydrogenate to the corresponding imines (**Scheme 1**, **1a**–**13a**). To our delight, benzyl anilines bearing different functional groups were successfully converted to their corresponding imines in good to excellent yields. For example, thioether (**3a**), alkynyl (**5a**), carboxylic acid ester (**7a**), boronic acid ester (**8a**), nitro (**9a**), nitrile (**11a**) and hydroxyl (**12a**) groups were well tolerated and dehydrogenated with an excellent yield. In addition to these, electron-donating (**2**–**5a**) and electron-withdrawing groups (**9**–**11a**) or both of them in a single molecule (**6a**) reacted excellently under the optimized reaction conditions. Moreover, the catalyst was able to dehydrogenate an aliphatic benzylic amine (**13a**) to the corresponding imine in an excellent yield under optimized reaction conditions. It should be noted that compound **4b** and **6b** have been used as intermediates for the syntheses of pyrrolidinone and piperidinone derivatives for urokinase receptor binding studies.[15] Additionally, acyclic imines (**13 b**) can be used for the synthesis of artificial amino acids.[16]

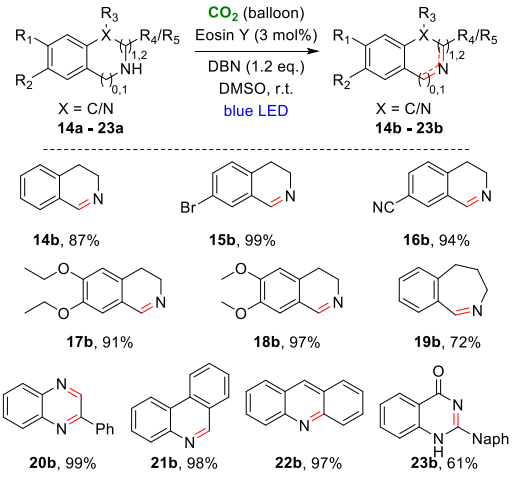

Reaction conditions: Substrate (0.134 mmol), eosin Y (3 mol%), DBN (1.2 eq), DMSO (2.5 mL), CO_2 (balloon), 12 W blue LED, r.t., 48 h. All are isolated yields.

Scheme 2. Substrates scope for the CO_2-catalyzed dehydrogenation of cyclic amines

After successfully dehydrogenating the acyclic amines, we became interested in cyclic amines (**Scheme 2**, **14a**–**23a**). In case of 1,2,3,4-tetrahydroisoquinoline derivatives, catalyst was able to dehydrogenate substrates bearing electron-withdrawing (**15**–**16a**) as well as electron-donating groups (**17**–**18a**) to the corresponding 3,4-dihydroisoquinoline derivatives in high yields. In case of 2-phenyl-2,3-dihydro-quinoxaline derivative (**20a**), formation of the doubly dehydrogenated product was observed in quantitative yield. We believed that the driving force for this reaction was the aromatization to the conjugated π-system of the product. In addition to these, different ring size (**19a**) and condensed ring systems (**21**–**22a**) reacted in good to high yields. Under this condition, an amide group was also tolerated (**Scheme 2**, **23a**). Finally, we became interested to dehydrogenate 1,2,3,6,7,11*b*-hexahydro-4*H*-pyrazino[2,1-*a*] *iso*-quinolin-4-one (**Scheme 3**) and we were pleased to observe the dehydrogenation of the C–C bond between 1- and 2-position in good yield. It is noteworthy that in none of the cases any byproduct or further dehydrogenation to the isoquinoline derivative was observed. Traditionally, these imines can be synthesized by the Bischler-Napieralski reaction employing toxic $POCl_3$ in stoichiometric amount. Compared to this, CO_2-catalysed methodology provide a simple, environment friendly and less toxic route with a metal-free way to this widely applicable imines. Additionally, partially dehydrogenated 3,4-dihydroisoquinoline derivatives have been

used for the syntheses of isoquinoline alklaoids such as **18b** has been used in the synthesis of berine.[17]

Reaction conditions: Substrate (0.134 mmol), eosin Y (3 mol%), DBN (1.2 eq.), DMSO (2.5 mL), CO_2 (balloon), 12 W blue LED, r.t., 48 h; isolated yield.

Scheme 3. Dehydrogenation of 1,2,3,6,7,11*b*-hexahydro-4*H*-pyrazino[2,1-*a*]isoquinolin-4-one

Since indole derivatives are important structural motifs found in many natural products (e.g. tryptophan and tryptamine alkaloids) and drug molecules (e.g. indometacin), our efforts were also paid to dehydrogenate a variety of indoline derivatives to achieve corresponding indole derivatives (**Scheme 4**, **25a–31a**).[18] Unsubstituted indoline (**25a**) reacted excellently and 79% of indole was isolated. In addition to this, substituted indoline derivatives (**26a–30a**) gave excellent yields of more than 90%. The catalyst was also tolerant towards carboxylic acid group (**29a**) and heteroaromatic indoline derivatives (**30a–31a**). No other by-products were identified in these reactions and in case of **30a**, we observed the double dehydrogenation to attain the aromaticity in the product.

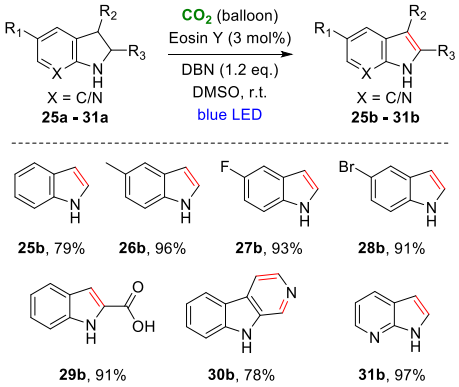

Reaction conditions: Substrate (0.134 mmol), eosin Y (3 mol%), DBN (1.2 eq.), DMSO (2.5 mL), CO_2 (balloon), 12 W blue LED, r.t., 48 h. All are isolated yields.

Scheme 4. Substrates scope for the dehydrogenation of indoline derivatives to indole derivatives

The aromatization of Hantzsch ester-type molecules is also important to synthesize poly-substituted pyridine derivatives. Ideally, these Hantzsch ester-type molecules can be synthesized *via* condensation reactions and further dehydrogenation to these should generate desired pyridine derivatives (**Scheme 5**, **32a–35a**).[19] Therefore, we examined our catalyst for the dehydrogenation of these types of molecules and to our delight, ethyl (**32a**) and *tert*-butyl ester (**33a**) as well as others (**34a–35a**) have shown excellent reactivity and quantitative products were isolated after 16 h of the reaction.

Additionally, the catalyst was able to show the condensation of aromatic diamines with aldehydes under our optimized conditions with an *in situ* dehydrogenation/aromatization of the formed 5- and 6-membered ring (**Scheme 6**). This condensation reaction is known to proceed at room temperature within 24-60 h.[20] However, under our reaction conditions the condensation was not only proceeded within 16 h but was also able to attain high yields of the *in situ* dehydrogenated products from 4-methylbenzaldehyde, furfural and isonicotinaldehyde (**36a – 38a**).

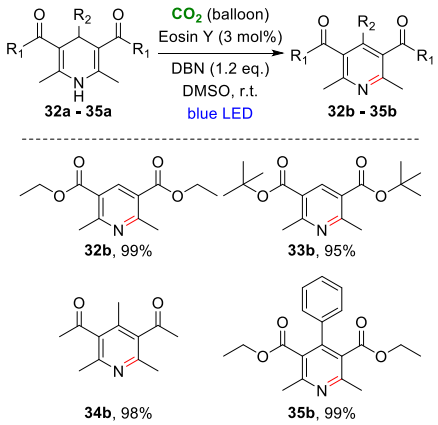

Reaction conditions: Substrate (0.134 mmol), eosin Y (3 mol%), DBN (1.2 eq.), DMSO (2.5 mL), CO_2 (balloon), 12 W blue LED, r.t., 16 h. All are isolated yields.

Scheme 5. CO_2-catalyzed syntheses of poly-substituted pyridine derivatives

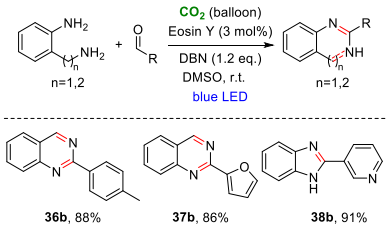

Reaction conditions: Substrate (0.134 mmol), eosin Y (3 mol%), DBN (1.2 eq.), DMSO (2.5 mL), CO_2 (balloon), 12 W blue LED, r.t., 16 h. All are isolated yields.

Scheme 6. Condensation of diamines and aldehydes and *in situ* oxidation to the heteroaromatic derivatives

Finally, we became keen on finding applications of this CO_2-catalyzed metal-free dehydrogenation reactions towards pharmaceutical molecules. For this purpose, we were interested to synthesize harmine (**39b**), a well-known monoamine inhibitor which also possesses anti-HIV and anti-tumor active properties.[21] Our interest was also to synthesize dehydronifedipine (**40b**), an active metabolite (metabolized by the cytochrome P450 isomers CYP3A4 and CYP3A5) and the actual active agent for anti-hypertensive treatment.[22] In fact, our catalyst selectively synthesized these two drugs up to 74% yield using catalytic amount of CO_2 (20 mol%) (**Scheme 7**).

After developing excellent substrates scope, we investigated the reaction mechanism of this CO_2-catalyzed dehydrogenation reaction. Initially, we carried out control experiments of the model substrate with radical quenchers (**Table 1**). To our delight, the reaction showed lower activity under oxygen and nitrogen atmosphere. The reaction did not

show any activity without the presence of light source, base or the catalyst which clearly depicted distinct role of CO_2, catalyst, base and light source in this reaction. Inactivity under

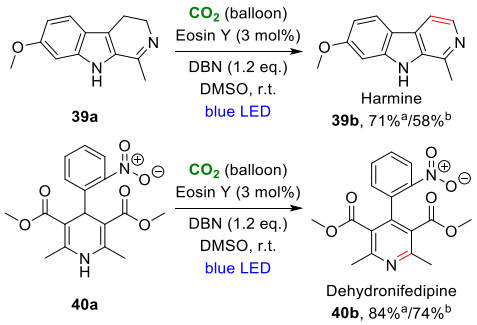

Reaction conditions: Substrate (0.134 mmol), eosin Y (3 mol%), DBN (1.2 eq.), DMSO (2.5 mL), 12 W blue LED, r.t., 16–40 h. All are isolated yields: [a]CO_2 balloon, [b]20 mol% CO_2.

Scheme 7. CO_2-catalyzed synthesis of harmine and dehydronifedipine drug molecules

O_2 atmosphere ruled out that traces of oxygen in the reaction could be the actual oxidant. Furthermore, different radical quenchers such as butylated hydroxytoluene (BHT) and (2,2,6,6-tetramethylpiperidin-1-yl)oxyl (TEMPO) showed low to no activity (**Table 1**, entries 6–9) which indicated a radical pathway. The reaction was also quenched in the presence of benzoquinone which could be because of the presence of carbon dioxide radical anion as there was no presence of oxygen in the system.[23]

Table 1. Mechanistic experiments: different CO_2 amounts and control experiments

Entry	Changed reaction parameter	Yield [%]
1	O_2 balloon*	5
2	N_2 atmosphere*	1
3	no light	0
4	no Eosin Y	0
5	no base	0
6	0.2 eq. BHT	12
7	1.0 eq. BHT	0
8	0.2 eq. TEMPO	0
9	1.0 eq. TEMPO	0
10	Benzoquinone	2

Reaction conditions: Substrate (0.134 mmol), eosin Y (3 mol%), DBN (1.2 eq.), DMSO (2.5 mL), CO_2 (balloon), 12 W blue LED, rt, 48 h. Yields were determined by GC using *n*-dodecane as internal standard. *No CO_2 was present in this reaction.

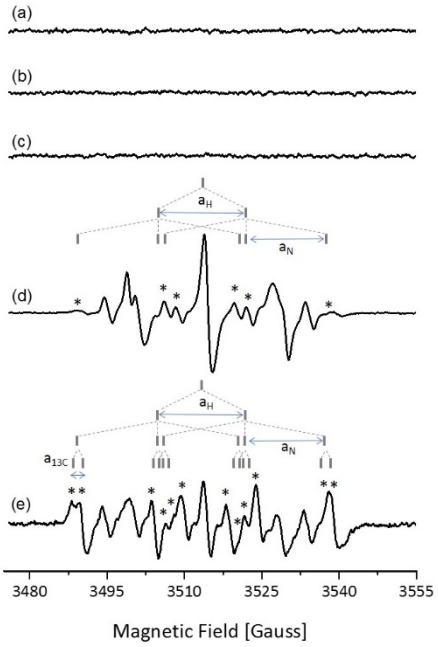

Description of different spectra: (a) N_2 atmosphere, DMPO/DMSO (54 mM), no light; (b) N_2 atmosphere, DMPO/DMSO (54 mM), eosin Y (3 mol%), DBN (1.2 eq.), substrate (0.134 mmol), blue LED light (18 h); (c) $^{12}CO_2$ atmosphere (balloon), DMPO/DMSO (54 mM), eosin Y (3 mol%), DBN (1.2 eq.), substrate (0.134 mmol), no light; (d) $^{12}CO_2$ atmosphere (balloon), DMPO/DMSO (54 mM), eosin Y (3 mol%), substrate (0.134 mmol), DBN (1.2 eq.), blue LED light for 18 h; (e) $^{13}CO_2$ atmosphere, DMPO/DMSO (54 mM), eosin Y (3 mol%), substrate (0.134 mmol), DBN (1.2 eq.), blue LED light for 18 h. The distinctive hf-lines of $^{12}CO_2$- and $^{13}CO_2$-centered subspectra in d) and e) are marked by stars. Experimental conditions: Bruker ElexSys E500 CW/Transient X-band EPR spectrometer equipped with the Bruker SHQ (ER4122 SHQE-W1) resonator, microwave frequency 9.87 GHz, microwave power 20 mW, field modulation 1 G, receiver gain 60 dB; conversion time 5.18 ms, number of averaged scans 400 and 81 for (a)-(c) and (d)-(e), respectively.

Chart 1. X-band EPR and background spectra of DMPO+CO_2 adducts measured under different conditions using DMPO as a trapping agent

This result triggered us to detect the radical by EPR spectroscopy using DMPO as radical trap. Indeed, after a blue LED light irradiation under reaction conditions (**Chart 1**), several DMPO adducts were created and observed by EPR. Their spectral lines overlap and make up the observed EPR spectra (**Chart 1** (d, e)). The radical spectra were only detected if the reaction conditions were fulfilled (compare **Chart 1** (a-c)). All species exhibited partially resolved hyperfine (hf) patterns mainly due to an internal interaction of the electron spin with the ^{14}N (I = 1) and β-^{1}H (I = ½) magnetic nuclei, which is typical for most DMPO adducts.[24] However, decay times of the contributing spectra were different, therefore systematic studies were obscured. Furthermore, due to an increased viscosity of the reaction mixture, correlation times of the observed adducts were prolonged, hence anisotropic contributions were visible and led to a deviation from isotropic-limit values. This feature further complicated the analysis of the contributing (sub)spectra. Thus, the exact assignment of the adducts is still ambiguous and should be a matter of further special studies.

However, the initial examination revealed that the hf structure of one of the subspectra (**Chart 1** (d), marked by stars) is in close agreement with the previously reported data for CO_2-centered DMPO radical adduct.[25] Furthermore, performing the reaction under $^{13}CO_2$ atmosphere led to an additional splitting of the hf-lines (**Chart 1** (e), stars), as expected due to an internal hf interaction with the magnetic ^{13}C isotope (I = ½). The effect should further support the CO_2 nature of the observed subspectrum contributing to the total EPR signal.

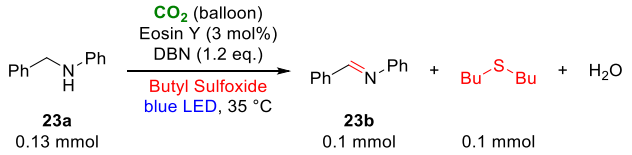

Reaction conditions: Substrate (0.134 mmol), eosin Y (3 mol%), DBN (1.2 eq.), DMSO (2.5 mL), CO_2 (balloon), 12 W blue LED, 35 °C, 48 h. Yield of **23b** was determined by GC using *n*-dodecane as internal standard; amount of $(n\text{-Bu})_2S$ was determined *via* GC-MS.

Scheme 8. Reaction of benzyl aniline in dibutyl sulfoxide as solvent

Additionally, no reduced products from CO_2 such as CO, HCO_2H or HCO_2^- were detected either by gas-phase GC analysis (see Supporting Information, **Chart S2**) or NMR spectroscopy and only CO_2 was observed in gas phase GC measurements. In order to find the actual oxidant and to quantify the reduced product in this reaction, dibutyl sulfoxide was chosen as solvent instead of DMSO (**Scheme 8**). The reduced product from dibutyl sulfoxide was dibutyl sulfide which was easier to quantify due to its high boiling point compared to DMS (188 °C and 37 °C, respectively). Analysis of the reaction mixture via GC and GC-MS clearly showed the evidence of the solvent being the actual oxidant and forming the corresponding dibutyl sulfide.

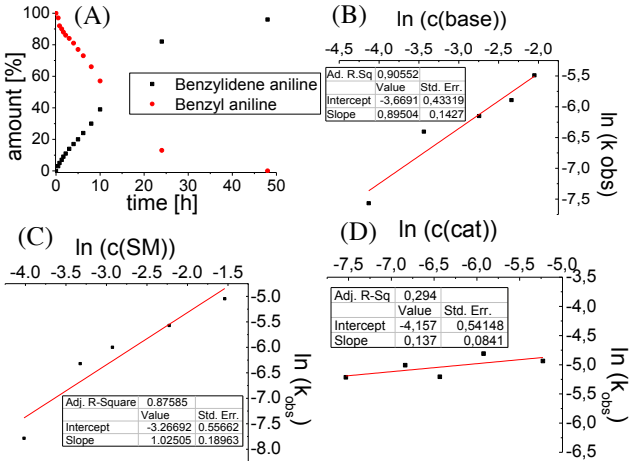

Chart 2. Reaction of benzyl aniline under optimized reaction conditions: Reaction was monitored over 48 h (A), plots for determination of reaction order with respect to DBN (B), benzyl aniline (C) and eosin Y (D)

Furthermore, we monitored the process of the model reaction over 48 h (**Chart 2, A**) and carried out experiments with different concentrations of DBN (**Chart 2, B**), benzyl aniline (**Chart 2, C**) and eosin Y (**Chart 2, D**). The concentrations were plotted against the observed rate constants in logarithmic way in order to determine the reaction order and it was found that the order of the reaction was 1st order with respect to DBN, benzyl aniline and 0th order with respect to the catalyst.

Further investigation by Stern-Volmer fluorescence quenching experiments revealed that the excited state of the photocatalyst was not quenched by carbon dioxide but rather by the amine (**Chart 3**).[26] Fluorescence intensity decreased with the increase of amine concentration and no change was observed with saturated carbon dioxide solution which clearly showed that the catalyst after excitation reacted with the starting material first but not with CO_2.

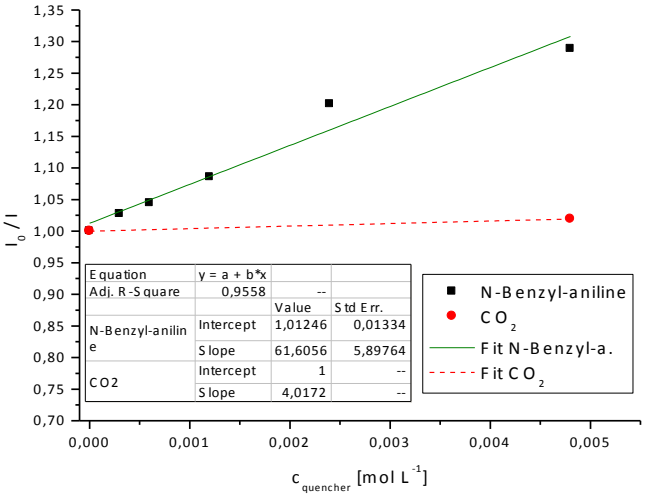

Chart 3. Stern-Volmer plot for eosin Y with benzyl aniline and CO_2 as potential quenchers

In order to find the rate-determining step, we also carried out KIE experiments (result of three independent runs each; **Scheme 9**) with mono- and di-deuterated **1a** which resulted in an average KIE of 1.3 for this reaction. This value clearly implied that the C–H bond cleavage of the starting material was the rate-determining step in this reaction. Additionally, D_2O peak was observed as the by-product in ^2H NMR spectra recorded from the reaction mixture of **1a-*d*$_2$** in non-deuterated DMSO (see Supporting Information, **Chart S3**).

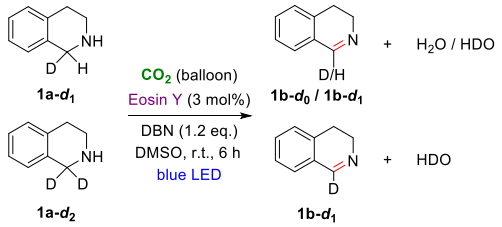

Reaction conditions: Substrate (0.134 mmol), eosin Y (3 mol%), DBN (1.2 eq.), DMSO (2.5 mL), CO_2 (balloon), 12 W blue LED, rt, 6 h. All are isolated yields.

Scheme 9. KIE experiment with mono- and di-deuterated substrate **1a**

Since the presence of CO_2 is necessary for the reaction to occur, we focused on the possible role of this molecule. CO_2 should be involved in the reductive part of the reaction mechanism, identifying the species, which is the energetically most favorable in the reaction mixture to be reduced should reveal the reaction mechanism and the role of the gas within.

Hence, we performed density functional theory and *ab initio* calculations with the COSMO-RS solvent model for DMSO to calculate the standard redox potential of five different species (**Chart 4**, for the description of the methods see the experimental section). The reduction of CO_2 to its radical anion exhibits a substantial redox potential of –2.79 V, which is in reasonable agreement the data of –2.21 V in literature.[4i] Since eosin Y has been shown to overcome only an approximately –1.06 V potential to reduce any molecule, it is difficult to interpret the reactions above through a free CO_2 radical anion.[27] Another possible species in the solution is the base, which was found to have an even higher redox potential, rendering the corresponding reduction also unlikely to play any role in the reaction. However, the strong base DBN can be protonated in the solution, which introduces a positive charge into the molecule. The charge decreases the redox potential significantly, and in the light of the overestimation of the redox potential for CO_2 above, it seems possible, although not likely that the protonated base is reduced by the eosin Y.

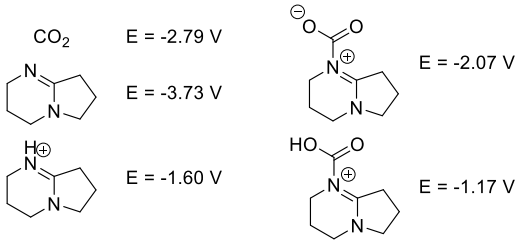

Chart 4. Calculated redox potentials of the species that may occur in the reaction mixture and the values are given for the reduction by a single electron

Being a Lewis acid, CO_2 is generally prone to react with bases. With DBN, we obtained a $\Delta G = -0.5$ kcal mol^{-1} reaction Gibbs free energy to form from free CO_2 and DBN a DBN-CO_2 adduct. For the resulting structure a somewhat less negative potential was found than for CO_2 or for free DBN, but notably more negative than for the protonated DBN. The DBN-CO_2 adduct is however possible to undergo protonation, resulting in structure DBN-CO_2H. This structure was found to have a redox potential of –1.17 V, which is the lowest value obtained here. The difference between this value and the literature data for eosin Y's reducing ability is well within the expected error of the applied computational methods. Accordingly, the reduction of the CO_2 to a radical anion is apparently aided by the DBN, which is in good agreement with the experimental results that the base is necessary for the reaction to occur. Since DBN is a stronger base than DBN-CO_2, it is reasonable to question the accessibility of DBN-CO_2H in the excess of DBN. The Gibbs free energy difference for the proton transfer from the protonated DBN to DBN-CO_2 was found to be only $\Delta G = 8.2$ kcal mol^{-1}, which is an energy demand that is possible to overcome at room temperature. This energy demand is easily compensated at the reduction process, which results in a $\Delta G = -9.9$ kcal mol^{-1} more stable product in case of DBN-CO_2H as compared to protonated DBN. This DBN-CO_2H adducts should be prone to degrade under reaction conditions when water is present. In fact, the product formation was increased using dry DBN (see **Table S1**). Additionally, formation of DBN-bicarbonate salt in the presence of water (which is apparent in commercial DBN) and the formation of carbamate anions from the respective starting material under CO_2 atmosphere were confirmed experimentally.[3c] These species may have some role in the mechanism which is a matter of further studies.

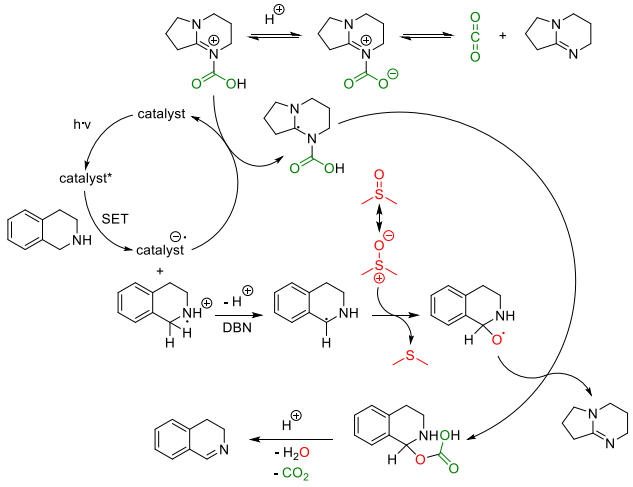

Scheme 10. Proposed reaction mechanism

Combining all the mechanistic experiments and calculations of the redox processes above, a complete mechanistic picture can be compiled (**Scheme 10**). First, the catalyst reaches the excited state by the irradiation of light. In the subsequent single electron transfer (SET) from the amine substrate an amine radical cation results, while the catalyst becomes a radical anion. The radical cation is then deprotonated by the base, and subsequently reacts with the DMSO to give an oxo radical species, and a DMS side product, in agreement with the observed reduction of the S=O bond in the control experiments with dibutyl sulfoxide. Although this step of the reaction was found to be endothermic in the calculations ($\Delta G = 26.6$ kcal mol^{-1}), the evaporation of DMS from the reaction mixture clearly shifts the energetics of this step in a manner that it becomes more favorable, which is in agreement with the longer reaction time necessary when dibutyl sulfoxide is used. Since the reaction needs at least 16 h to generate the product in considerable yields it is more likely to overcome this energetic barrier.

The catalyst radical anion reduces the DBN-CO_2H adduct, which yields the corresponding radical and the catalyst. The former species, which can be rationalized as a stabilized CO_2 radical anion, can recombine with the oxo radical derivative by transferring the ·CO_2H (hydroxycarbonyl radical) unit to the oxygen atom from the DBN-CO_2H radical to yield an alkyl carbonate in a highly exothermic reaction ($\Delta G = -67.4$ kcal mol^{-1}). This energetically downhill step also helps to overcome the energetic barrier in the previous step ($\Delta G = 26.6$ kcal mol^{-1}) to shift the reaction equilibrium to the product side. This structure can decompose to CO_2, water and the product in a thermodynamically favorable step ($\Delta G = -0.8$ kcal mol^{-1}). In fact, the water and CO_2 were both detected experimentally by ^{2}H NMR and gas GC measurements, respectively.

CONCLUSION

In conclusion, we have described the CO_2-catalyzed dehydrogenation of amines to imines. This metal-free catalytic system has shown broad substrates scope and excellent functional group tolerances. The application of this

methodology has been also described for the syntheses of pharmaceuticals. The generation of hydroxycarbonyl radical was confirmed by EPR spectroscopy. Several experiments have been done to have clear role of the catalyst and CO_2 in this reaction. Finally, detail mechanistic, kinetic and DFT calculations revealed the mechanism of this reaction.

ASSOCIATED CONTENT

Supporting Information. The Supporting Information contains technical details of the quantum chemical calculations, experimental details, characterization data and spectra of the synthesized compounds. This material is available free of charge via the Internet at http://pubs.acs.org.

AUTHOR INFORMATION

Corresponding Author

* Dr. Shoubhik Das (shoubhik.das@chemie.uni-goettingen.de)

Author Contributions

The manuscript was written through contributions of all authors. All authors have given approval to the final version of the manuscript.

Funding Sources

We thank Fonds der Chemischen Industrie (FCI, Liebig-Fellowship to S.D.) and Chinese Scholarship Council (CSC fellowship to Y.Z.) for the financial support.

ACKNOWLEDGMENTS

We are thankful to Prof. Dr. Lutz Ackermann for his support. Support from Prof. Dr. Inke Siewert for GC measurements is also acknowledged. We are also thankful to Prof. Dr. Marina Bennati for the support behind EPR spectroscopy.

ABBREVIATIONS

BHT, butylated hydroxytoluene; DBN, 1,5-diazabicyclo[4.3.0]non-5-ene; DBU, 1,8-diazabicyclo[5.4.0]undec-7-ene; DMS, dimethyl sulfide; DMSO, dimethyl sulfoxide; GC, gas chromatography; GC-MS, gas-chromatography-coupled mass spectroscopy; NMR, nuclear magnetic resonance; SET, single electron transfer; TBD, 1,5,7-triazabicyclo[4.4.0]dec-5-ene; TEMPO, 2,2,6,6-tetramethylpiperidin-1-yl)oxyl.

REFERENCES

[1] (a) Liu, Q.; Wu, L.; Jackstell, R.; Beller, M. Using carbon dioxide as a building block in organic synthesis. *Nat. Commun.* **2015**, *6*, 5933. (b) Artz, J.; Müller, T. E.; Thenert, K.; Kleinekorte, J.; Meys, R.; Sternberg, A.; Bradow, A.; Leitner, W. Sustainable Conversion of Carbon Dioxide: An Integrated Review of Catalysis and Life Cycle Assessment. *Chem. Rev.* **2018**, *118*, 434–504. (c) Aresta, M.; Dibenedetto, Angelini, A. Catalysis for the Valorization of Exhaust Carbon: from CO_2 to Chemicals, Materials, and Fuels. Technological Use of CO_2. *Chem. Rev.* **2014**, *114*, 1709–1742. (d) Klankermayer, J.; Wesselbaum, S.; Beydoun, K.; Leitner, W. Selective Catalytic Synthesis Using the Combination of Carbon Dioxide and Hydrogen: Catalytic Chess at the Interface of Energy and Chemistry. *Angew. Chem. Int. Ed.* **2016**, *55*, 7296–7343. (e) Li, Y.; Cui, X.; Dong, K.; Junge, K.; Beller, M. Utilization of CO_2 as a C1 Building Block for Catalytic Methylation Reactions. *ACS Catal.* **2017**, *7*, 1077–1086. (f) Bobbink, F. D.; Dyson, P. J. Synthesis of carbonates and related compounds incorporating CO_2 using ionic liquid-type catalysts: State-of-the-art and beyond. *J. Catal.* **2016**, *343*, 52–61. (g) Darensbourg, D. J. Making Plastics from Carbon Dioxide: Salen Metal Complexes as Catalysts for the Production of Polycarbonates from Epoxides and CO_2. *Chem. Rev.* **2007**, *107*, 2388–2410.

[2] (a) Oh, Y.; Hu, X. Organic molecules as mediators and catalysts for photocatalytic and electrocatalytic CO_2 reduction. *Chem. Soc. Rev.* **2013**, *42*, 2253–2261. (b) Costentin, C.; Robert, M.; Savéant, J.-M. Catalysis of the electrochemical reduction of carbon dioxide. *Chem. Soc. Rev.* **2013**, *42*, 2423–2436. (c) Izumi, Y. Recent advances in the photocatalytic conversion of carbon dioxide to fuels with water and/or hydrogen using solar energy and beyond. *Coord. Chem. Rev.* **2013**, *257*, 171–186. (d) Li, K.; Peng, B.; Peng, T. Recent Advances in Heterogeneous Photocatalytic CO_2 Conversion to Solar Fuels. *ACS Catal.* **2016**, *6*, 7485–7527. (e) Kuehnel, M. F.; Orchard, K. L., Dalle, K. E.; Reisner, E. Selective Photocatalytic CO_2 Reduction in Water through Anchoring of a Molecular Ni Catalyst on CdS Nanocrystals. *J. Am. Chem. Soc.* **2017**, *139*, 7217–7223. (f) Zhang, W.; Hu, Y.; Ma, L.; Zhu, G.; Wang, Y.; Xue, X.; Chen, R.; Yang, S.; Jin. Z. Progress and Perspective of Electrocatalytic CO_2 Reduction for Renewable Carbonaceous Fuels and Chemicals. *Adv. Sci.* **2018**, *5*, 1700275.

[3] (a) Fiorani, G.; Guo, W.; Kleij, A. W. Sustainable conversion of carbon dioxide: the advent of organocatalysis. *Green Chem.* **2015**, *17*, 1375–1389. (b) Gomes, C. D. N.; Jacquet, O.; Villiers. C.; Thuery, P.; Ephritikhine, M.; Cantat, T.; A Diagonal Approach to Chemical Recycling of Carbon Dioxide: Organocatalytic Transformation for the Reductive Funktionalization of CO_2. *Angew. Chem. Int. Ed.* **2012**, *51*, 187–190. (c) Riemer, D.; Hirapara, P.; Das, S. Chemoselective Synthesis of Carbamates using CO_2 as Carbon Source. *ChemSusChem* **2016**, *9*, 1916–1920. (d) Hulla, M.; Chama, S. A. M.; Laurenczy, G.; Das, S.; Dyson, P. J. Delineating the Mechanism of Ionic Liquids in the Synthesis of Quinazoline-2,4(1*H*,3*H*)-dione from 2-Aminobenzonitrile and CO_2. *Angew. Chem. Int. Ed.* **2017**, *56*, 10559–105693. (e) Hulla, M.; Bobbink, F. D.; Das, S.; Dyson, P. J. Carbon Dioxide Based *N*-Formylation of Amines Catalyzed by Fluoride and Hydroxide Anions. *ChemCatChem* **2016**, *8*, 3338–3342. (f) Bobbink, F. D.; Das, S.; Dyson, P. J. *N*-formylation and *N*-methylation of amines using metal-free *N*-heterocyclic carbene catalysts and CO_2 as carbon source. *Nat. Protocol* **2017**, *12*, 417–428. (g) Das, S.; Bobbink, F. D.; Laurenczy, G.; Dyson, P. J. Metal-free catalyst for the chemoselective methylation of amines using carbon dioxide as a carbon source. *Angew. Chem. Int. Ed.* **2014**, *53*, 12876–12879.

[4] (a) Luo, J.; Larrosa, I. C–H Carboxylation of Aromatic Compounds through CO_2 Fixation. *ChemSusChem* **2017**, *10*, 3317–3332. (b) Tommasi, I. Direct Carboxylation of $C(sp^3)$–H and $C(sp^2)$–H Bonds with CO_2 by Transition-Metal-Catalyzed and Base-Mediated Reactions. *Catalysts* **2017**, *7*, 380. (c) Börjesson, M.; Moragas, T.; Gallego, D.; Martin, R. Metal-Catalyzed Carboxylation of Organic (Pseudo)halides with CO_2. *ACS Catal.* **2016**, *6*, 6739–6749. (d) Ackermann, L. Transition-metal-catalyzed carboxylation of C–H bonds. *Angew. Chem. Int. Ed.* **2011**, *50*, 3842–2844. (e) Sasano, K.; Takaya, J.; Iwasawa, N. Palladium(II)-Catalyzed Direct Carboxylation of Alkenyl C–H Bonds with CO_2. *J. Am. Chem. Soc.* **2013**, *135*, 10954–10957. (f) Mizuno, H.; Takaya, J.; Iwasawa, N. Rhodium(I)-Catalyzed Direct Carboxylation of Arenes with CO_2 via Chelation-Assisted C–H Bond Activation. *J. Am. Chem. Soc.* **2011**, *133*, 1251–1253. (g) Masuda, Y.; Ishida, N.; Murakami, M. Light-Driven Carboxylation of *o*-Alkylphenyl Ketones with CO_2. *J. Am. Chem. Soc.* **2015**, *137*, 14063–14066. (h) Meng, Q.; Wang, S.; König, B. Carboxylation of Aromatic and Aliphatic Bromides and Triflates with CO_2 by Dual Visible-Light-Nickel Catalysis. *Angew. Chem. Int. Ed.* **2017**, *56*, 13426–13430. (i) Seo, H.; Katcher, M. H.; Jamison, T. F. Photoredox activation of carbon dioxide for amino acid synthesis in continuous flow. *Nat. Chem.* ***2017, 9,*** 453–456. (j) Michigani, K.; Mita, T.; Sato, Y. Cobalt-Catalyzed Allylic $C(sp^3)$–H Carboxylation with CO_2. *J. Am. Chem. Soc.* **2017**, *139*, 6094–6097. (k) Banerjee, A.; Dick, G. R.; Yoshino, T.; Kanan, M. W. Carbon dioxide utilization via carbonate-promoted C–H carboxylation. *Nature* **2016**, *531*, 215–219.

[5] (a) Sugawara, Y.; Yamada, W.; Yoshida, S.; Yamada, T. Carbon Dioxide-Mediated Catalytic Rearrangement of Propargylic Alcohols into *α,β*-Unsaturated Ketones. *J. Am. Chem. Soc.* **2007**, *129*, 12902–12903. (b) Ansari, M. B.; Park, S.-E. Carbon dioxide utilization as a soft oxidant and promoter in catalysis. *Energy. Environ. Sci.* **2012**, *5*, 9419–9437. (c) Ansari, M. B.; Min, B.-H.; Mo Y.-H., Park, S.-E. CO_2 activation and promotional effect in the oxidation of cyclic olefins over mesoporous carbon nitrides. *Green Chem.* **2011**, *13*, 1416–1421. (d) Zhang, L.; Wu, Z.; Nelson, N. C.; Sadow, A. D.; Slowing, I. I.; Overbury, S. H. Role Of CO_2 As a Soft Oxidant For Dehydrogenation of Ethylbenzene to Styrene over a High-Surface-Area Ceria Catalyst. *ACS Catal.* **2015**, *5*, 6426–6435. (e) Ma, R.; Liu, A. -H.; Huang, C. -B.;

Li, X. -D.; He, L. N. Reduction of sulfoxides and pyridine-*N*-oxides over iron powder with water as hydrogen source promoted by carbon dioxide. *Green Chem.* **2013**, *15*, 1274–1279. (f) He, H.; Qi, C.; Hu, X.; Guan, Y.; Jiang, H. Efficient synthesis of tertiary *α*-hydroxy ketones through CO_2-promoted regioselective hydration of propargylic alcohols. *Green Chem.* **2014**, *16*, 3729–3733. (g) Lee, R.; Harris, J.; Champagne, P.; Jassop, P. G. CO_2-Catalysed conversion of carbohydrates to 5-hydroxymethyl furfural. *Green Chem.* **2016**, *18*, 6305–6310. (h) Pupo, G.; Properzi, R.; List, B. Asymmetric Catalysis with CO_2: The Direct *α*-Allylation of Ketones. *Angew. Chem. Int. Ed.* **2016**, *55*, 6099–6102. (i) Kapoor, M.; Liuz, D.; Young, M. C. Carbon Dioxide-Mediated C(sp^3)–H Arylation of Amine Substrates. *J. Am. Chem. Soc.* **2018**, *140*, 6818–6822. (j) Schilling, W.; Das, S. CO_2-catalysed/promoted transformation of organic functional groups. *Tetrahedron Lett.* **2018**, *59*, 3821-3828.

[6] (a) Riemer, D.; Mandaviya, B.; Schilling, W.; Götz, A. C.; Kühl, T.; Finger, M.; Das, S. CO_2-Catalyzed Oxidation of Benzylic and Allylic Alcohols with DMSO. *ACS Catal.* **2018**, *8*, 3030–3034. (b) Hirapara, P.; Riemer, D.; Hazra, N.; Gajera, J.; Finger, M.; Das, S. CO_2-assisted synthesis of non-symmetric α-diketones directly from aldehydes *via* C–C bond formation. *Green Chem.* **2017**, *19*, 5356–5360.

[7] (a) Layer, R. W.The Chemistry of Imines. *Chem. Rev.* **1963**, *63*, 489–510. (b) Patil. R. D.; Adimurthy, S. Catalytic Methods for Imine Synthesis. *Asian. J. Org. Chem.* **2013**, *2*, 726–744. (c) Martin, S. F. Recent applications of imines as key intermediates in the synthesis of alkaloids and novel nitrogen heterocycles. *Pure Appl. Chem.* **2009**, *81*, 195–204. (d) Belowich, M. E.; Stoddart, J. F.; Dynamic imine chemistry. *Chem. Soc. Rev.* **2012**, *41*, 2003–2024. (e) Dai, L.; Lin, Y.; Hou, X.; Zhou, Y. Stereoselective reactions with imines. *Pure Appl. Chem.* **1999**, *71*, 1033–1040. (f) Zhou, S.; Fleischer, S.; Junge, K.; Das, S.; Addis, D.; Beller. M. Enantioselective Synthesis of Amines: General, Efficient Iron-Catalyzed Asymmetric Transfer Hydrogenation of Imines. *Angew. Chem. Int. Ed.* **2010**, *49*, 8121–8125. (g) Wendlandt, A. E.; Stahl, S. S. Modular *o*-Quinone Catalyst System for Dehydrogenation of Tetrahydroquinolines under Ambient Conditions. *J. Am. Chem. Soc.* **2014**, *136*, 11910–11913. (h) Wendlandt, A. E.; Stahl, S. S. Bioinspired Aerobic Oxidation of Secondary Amines and Nitrogen Heterocycles with a Bifunctional Quinone Catalyst. *J. Am. Chem. Soc.* **2014**, *136*, 506–512.

[8] (a) Cole, E. B.; Lakkaraju, P. S.; Rampulla, D. M.; Morris, A. J.; Abelev, E.; Bocarsly, A. B. Using a One-Electron Shuttle for the Multielectron Reduction of CO_2 to Methanol: Kinetic, Mechanistic, and Structural Insights. *J. Am. Chem. Soc.* **2010**, *132*, 11539–11551. (b) Boston, D. J.; Xu, C.; Armstrong, D. W.; MacDonnell, F. M. Photochemical Reduction of Carbon Dioxide to Methanol and Formate in a Homogeneous System with Pyridinium Catalysts. *J. Am. Chem. Soc.* **2013**, *135*, 16252–16255.

[9] (a) Seo, H.; Liu, A.; Jamison, T. F. Direct *β*-Selective Hydrocarboxylation of Styrenes with CO_2 Enabled by Continuous Flow Photoredox Catalysis. *J. Am. Chem. Soc.* **2017**, *139*, 13969–13972. (b) Morgenstern, D. A.; Wittrig, R. E.; Fanwick, P. E.; Kubiak, C. P. Photoreduction of carbon dioxide to its radical anion by nickel cluster $[Ni_3(\mu_3\text{-}I)_2(dppm)_3]$: Formation of Two Carbon–Carbon Bonds *via* Addition of CO_2^- to Cyclohexene. *J. Am. Chem. Soc.* **1993**, *115*, 6740–6471. (c) Akhgarnusch, A.; Höckendorf, R. F.; Hao, Q.; Jäger, K. P.; Siu, C.; Beyer, M. K. Carboxylation of methyl acrylate by carbon dioxide radical anions in gas-phase water clusters. *Angew. Chem. Int. Ed.* **2013**, *52*, 9327–9330.

[10] (a) Perez, E. R.; Santos, R. H. A.; Gambardella, M. T. P.; de Macedo, L. M.; Rodrigues-Filho, U. P.; Launay, J.-C.; Franco, D. W. Activation of Carbon Dioxide by Bicyclic Amidines, *J. Org. Chem.* **2004**, *69*, 8005–8011. (b) Heldebrant, D. J.; Jessop, P. G.; Thomas, C. A.; Eckert, C. A.; Liotta, C. L. The Reaction of 1,8-Diazabicyclo[5.4.0]undec-7-ene (DBU) with Carbon Dioxide. *J. Org. Chem.* **2005**, *70*, 5335–5338.

[11] (a) Ji, X.; Su, Z.; Wang, P.; Ma, G.; Zhang, S. Integration of Artificial Photosynthesis System for Enhanced Electronic Energy-Transfer Efficacy: A Case Study for Solar-Energy Driven Bioconversion of Carbon Dioxide to Methanol. *Small* **2016**, *12*, 4753–4762. (b) Kuk, S. K.; Singh, R. K.; Nam, D. H.; Singh, R.; Lee, J.-K.; Park, C. B. Photoelectrochemical Reduction of Carbon Dioxide to Methanol through a Highly Efficient Enzyme Cascade. *Angew. Chem. Int. Ed.* **2017**, *56*, 3827–3832.

[12] (a) Iosub, A. V.; Stahl, S. S. Catalytic Aerobic Dehydrogenation of Nitrogen Heterocycles Using Heterogeneous Cobalt Oxide Supported on Nitrogen-Doped Carbon, *Org. Lett.* **2015**, *17*, 4404−4407. (b) Choi, H.; Doyle, M. P. Oxidation of secondary amines catalyzed by dirhodium caprolactamate, *Chem. Commun.* **2007**, 745–747.

[13] (a) Samec, J. M. S.; Éll, A. H.; Bäckvall, J.-E. Efficient Ruthenium-Catalyzed Aerobic Oxidation of Amines by Using a Biomimetic Coupled Catalytic System, *Chem. Eur. J.* **2005**, *11*, 2327 – 2334. (b) So, M.-H.; Liu, Y.; Ho, C.-M.; Che, C.-M. Graphite-Supported Gold Nanoparticles as Efficient Catalyst for Aerobic Oxidation of Benzylic Amines to Imines and *N*-Substituted 1,2,3,4-Tetrahydroisoquinolines to Amides: Synthetic Applications and Mechanistic Study, *Chem. Asian J.* **2009**, *4*, 1551–1561. (c) Wang, J.-R.; Fu, Y.; Zhang, B.-B.; Cui, X.; Liu, L.; Guo, Q.-X. Palladium-catalyzed aerobic oxidation of amines, *Tetrahedron Lett.* **2006**, *47*, 8293–8297.

[14] (a) Jin, Y.; Ou, L.; Yang, H.; Fu, H. Visible-Light-Mediated Aerobic Oxidation of *N*-Alkylpyridinium Salts under Organic Photocatalysis. *J. Am. Chem. Soc.* **2017**, *139*, 14237–14243. (b) Romero, N.; Nicewicz, D. A. Organic Photoredox Catalysis. *Chem. Rev.* **2016**, *116*, 10075–10166. (c) Neumann, M.; Fuldner, S.; König, B.; Zeitler, K. Metal-Free, Cooperative Asymmetric Organophotoredox Catalysis with Visible Light. *Angew. Chem. Int. Ed.* **2011**, *50*, 951–954. (d) Romero, N. A.; Margrey, K. A.; Tay, N. E.; Nicewicz, D. A. Site-selective arene C–H amination *via* photoredox catalysis. *Science* **2015**, *349*, 1326–1330. (e) Ghosh, I.; Ghosh, T.; Bardagi, L. J.; König, B. Reduction of aryl halides by consecutive visible light-induced electron transfer processes. *Science*, **2014**, *346*, 725–728. (f) Schilling, W.; Riemer, D.; Zhang, Y.; Hatami, N.; Das, S. Metal-Free Catalyst for Visible-Light-Induced Oxidation of Unactived Alcohols Using Air/Oxygen as an Oxidant. *ACS Catal.* **2018**, *8*, 5425–5430. (g) Zhang, Y.; Riemer, D.; Schilling, W.; Kollmann, J.; Das, S. Visible-Light-Mediated Efficient Metal-Free Catalyst for *α*-Oxygenation of Tertiary Amines to Amides. *ACS Catal.* **2018**, *8*, 6659–6664.

[15] Mani, T.; Liu, D.; Zhou, D.; Li, L.; Knabe, W. E.; Wang, F.; Oh, K.; Meroueh, S. O. Probing Binding and Cellular Activity of Pyrrolidinone and Piperidinone Small Molecules Targeting the Urokinase Receptor, *ChemMedChem* **2013**, *8*, 1963–1977.

[16] Sathe, A. A.; Hartline, D. R.; Radosevich, A. T. A synthesis of α-amino acids *via* direct reductive carboxylation of imines with carbon dioxide, *Chem. Commun.* **2013**, *49*, 5040–5042.

[17] (a) Sasamoto, N.; Dubs, C.; Hamashima, Y.; Sodeoka, M. Pd(II)-Catalyzed Asymmetric Addition of Malonates to Dihydroisoquinolines, *J. Am. Chem. Soc.* **2006**, *128*, 14010-14011. (b) Itoh, T.; Miyazaki, M., Fukuoka, H.; Nagata, K.; Ohsawa, A. Formal Total Synthesis of (−)-Emetine Using Catalytic Asymmetric Allylation of Cyclic Imines as a Key Step, *Org. Lett.* **2006**, *8*, 1295–1297. (c) Szawkało, J.; Czarnock, Z. Enantioselective Synthesis of Some Tetracyclic Isoquinoline Alkaloids by Asymmetric Transfer Hydrogenation Catalysed by a Chiral Ruthenium Complex, *Monatsh. Chem.* **2005**, *136*, 1619–1627. (c) Kanemitsu, T.; Yamashita, Y.; Nagata, K.; Itoh, T. Catalytic Asymmetric Synthesis of (R)-(–)-Calycotomine, (S)-(–)-Salsolidine and (S)-(–)-Carnegine, *Synlett* **2006**, *10*, 1595–1597. (d) Hoye, T. R.; Chen, M. Total synthesis of (*ent*)-korupensamine D, *Tetrahedron Lett.* **1996**, *37*, 3099–3100. (e) Liu, L. Enantioselective Synthesis of Protoberberine Alkaloids *via* (–)-Sparteine-mediated Asymmetric Condensation-Cyclisation of *o*-Toluamide Anions with 3,4-Dihydroisoquinolines, *Synthesis* **2003**, *11*, 1705–1706.

[18] (a) Capim, S. L.; Gonçalves, G. M.; dos Santos, G. C. M.; Marinho, B. G. High analgesic and anti-inflammatory *in vivo* activities of six new hybrids NSAIAs tetrahydropyran derivatives. *Bioorg. Med. Chem.* **2013**, *21*, 6003–6010. (b) Arisawa, M., Kasaya, Y., Obata, T.; Sasaki, T.; Ito, M.; Abe, H.; Ito, Y.; Yamano, A.; Shto, S. Indomethacin Analogues that Enhance Doxorubicin Cytotoxicity in Multidrug Resistant Cells without Cox Inhibitory Activity. *ACS Med. Chem. Lett.* **2011**, *2*, 353–357. (c) Milen, M.; Ábrányi-Balogh, P. Synthesis of *β*-carbolines. *Chem. Heterocycl. Compd.* **2016**, *52*, 996–998. (d) Hibino, S.; Choshi, T. Simple indole alkaloids and those with a nonrearranged monoterpenoid unit. *Nat. Prod. Rep.* **2001**, *18*, 66–87.

[19] (a) Balogh, M.; Hermecz, I.; Mészáros, Z.; Laszlo, P. Aromatization of 1,4-Dihydropyridines by Clay-Supported Metal Nitrates. *Helv. Chim. Acta* **1984**, *67*, 2270–2272. (b) Khadilkar, B.; Borkar, S. Silica Gel Supported Ferric Nitrate: A Convenient Oxidizing Reagent. *Synth. Commun.* **1998**, *28*, 207–212. (c) Xia, J.-J.; Wang, G.-W. One-Pot Synthesis and Aromatization of 1,4-Dihydropyridines in Refluxing Water. *Synthesis* **2005**, *14*, 2379–2383. (c) Vanden Eynde, J.-J.; D'Orazio, R.; Haverbeke, Y. V. Potassium permanganate, a versatile reagent for the aromatization of Hantzsch 1,4-dihydropyridines. *Tetrahedron* **1994**, *50*, 2479–2484.

[20] Zhang, J.; Chen, S.; Chen, F.; Xu, W.; Deng, G.-J. Gong, H. Dehydrogenation of Nitrogen Heterocycles Using Graphene Oxide as a Versatile Metal-Free Catalyst under Air. *Adv. Synth. Catal.* **2017**, *359*, 2358–2363.

[21] (a) Kusurkar, R. S.; Goswami, S. K. Efficient one-pot synthesis of anti-HIV and anti-tumour *β*-carbolines. *Tetrahedron* **2004**, *60*, 5315–5318. (b) Eagon, S.; Anderson, M. O. Microwave-Assisted Synthesis of Tetrahydro-*β*-carbolines and *β*-carbolines. *Eur. J. Org. Chem.* **2014**, 1653–1665. (c) Wu, J.; Talwar, D.; Johnston, S.; Yan, M.; Xiao, J. Acceptorless Dehydrogenation of Nitrogen Heterocycles with a Versatile Iridium Catalyst. *Angew. Chem. Int. Ed.* **2013**, *52*, 6983–6987. (d) Wang, J.; Du, H.; Li, N.; Gu, H.; Liu, B. 2-substituted-beta-carboline compounds and application thereof in preparing drugs for preventing or treating tumors. Chin. Pat. 104557916, **2014**. (e) Wang, J.; Du, H.; Li, N.; Gu, H.; Qin, W. β-carboline compounds and salts of dimer for the preparation of medicament for preventing or treating tumors. Chin. Pat. 104497012, **2014**.

[22] (a) Choi, J.-S.; Choi, J. -S.; Choi, D.-H. Effects of licochalcone A on the bioavailability and pharmacokinetics of nifedipine in rats: possible role of intestinal CYP3A4 and P-gp inhibition by licochalcone A. *Biopharm. Drug Dispos.* **2014**, *35*, 382–390. (b) Ardizzone, T. D.; Lu, X.-H.; Dwyer, D. S. Calcium-independent inhibition of glucose transport in PC-12 and L6 cells by calcium channel antagonists. *Am. J. Phiosol. Cell Phiosol.* **2002**, *283*, C579–C583. (c) Zeynizadeh, B.; Dilmaghani, K. A.; Roozijoy, A. $KBrO_3/FeCl_3$ as an efficient oxidizing system for aromatization of Hantzsch 1,4-dihydropyridines in wet acetonitrile. *J. Chem. Res.* **2005**, *10*, 657–658. (d) Lemay, J.; Tea, B. S.; Hamet, P.; deBlois, D. Prevalence of deep venous anomalies in congenital vascular malformations of venous predominance. *J. Vasc. Res.* **2001**, *38*, 462–471. (e) Ago, T.; Yang, Y.; Zhai, P.; Sadoshima, J. Nifedipine inhibits cardiac hypertrophy and left ventricular dysfunction in response to pressure overload. *J. Cardiovasc. Transl. Res.* **2010**, *3*, 304–313. (f) Patki, K. C.; von Moltke, L. L.; Greenblatt, D. J. In vitro Metabolism of Midazolam, Triazolam, Nifedipine, and Testosterone by Human Liver Microsomes and Recombinant Cytochromes P450: Role of CYP3A4 and CYP3A5. *Drug Metab. Dispos.* **2003**, *31*, 938–944. (g) Wie, X.; Wang, L.; Jia, W.; Du, S.; Wu, L.; Liu, Q. Metal-Free-Mediated Oxidation Aromatization of 1,4-Dihydropyridines to Pyridines Using Visible Light and Air. *Chin. J. Chem.* **2014**, *32*, 1245–1250. (h), Lee, C.-K.; Choi, J.-S.; Choi, D.-H. Effects of Cilostazol on the Pharmacokinetics of Nifedipine After Oral and Intravenous Administration in Rats. *Pharm. Chem. J.* **2017**, *51*, 748–755. (i) Chaikh, A. C.; Chen, C. Facile and efficient aromatization of 1,4-dihydropyridines with $M(NO_3)_2{\cdot}XH_2O$, TNCB, TBAP and HMTAI and preparation of deuterium labeled dehydronifedipine from nifedipine-d_3. *Bioorg. Med. Chem. Lett.* **2010**, *20*, 3664–3668.

[23] Maurette, M.-T.; Oliveros, E.; Infelta, P. P.; Ramsteiner, K., Braun, A. M. Singlet Oxygen and Superoxide: Experimental Differentiation and Analysis. *Helv. Chim. Acta* **1983**, *66*, 722–733.

[24] Villamena, F. A.; Locigno, E. J.; Rockenbauer, A.; Hadad, C. M.; Zweier, J. L. Theoretical and Experimental Studies of the Spin Trapping of Inorganic Radicals by 5,5-Dimethyl-1-Pyrroline N-Oxide (DMPO). 1. Carbon Dioxide Radical Anion. *J. Phys. Chem. A*, **2006**, *110*, 13253–13258.

[25] (a) Tanigushi, H.; Madden, K. P. DMPO-Alkyl Radical Spin Trapping: An *In Situ* Radiolysis Steady-State ESR Study. *Radiat. Res.* **2000**, *153*, 447–453. (b) Kirino, Y.; Ohkuma, T.; Kwan, T. Spin Trapping with 5,5-Dimethylpyrroline-N-oxide in Aqueous Solution. *Chem. Pharm. Bull.* **1981**, *29*, 29–34.

[26] (a) Arias-Rotondo, D. M.; McCusker, J. K. The photophysics of photoredox catalysis: a roadmap for catalyst design. *Chem. Soc. Rev.* **2016**, *45*, 5803–5820. (b) Zhang, Y.; Riemer, D.; Schilling, W.; Kollmann, J.; Das, S. Visible-light-mediated efficient metal-free catalysts for α-oxygenation of tertiary amines to amide. *ACS Catal.* **2018**, *8*, 6659. (c) Schilling, W.; Riemer, D., Zhang, Y.; Hatami, N.; Das, S. Metal-free catalyst for visible-light-induced oxidation of unactivated alcohols using air/oxygen as an oxidant. *ACS Catal.* **2018**, *8*, 5425.

[27] Srivastava, V.; Singh, P. P. Eosin Y catalyzed photoredox sysnthesis: a review. *RSC Adv.* **2017**, *7*, 31377–31392.

Insert Table of Contents artwork here